Viscoelastic fluid effect on the surface wave propagation

Adil El Baroudi, Jean Yves Le Pommellec

Viscoelastic Fluid Effect on the Surface Wave Propagation

A. El Baroudi[a,*], J. Y. Le Pommellec[a]

[a] *Arts et Métiers ParisTech, 2 bd du Ronceray, 49035 Angers, France*

Abstract

A novel approach based on the exact theory has been developed to accurately predict the behavior of surface Love wave propagating in elastic waveguide loaded on its surface with a viscoelastic fluid. A detailed study was conducted by varying key parameters such as operating frequency, waveguide and substrate. The waveguide surface was subjected to various glycerol concentrations, with a wide range of dynamic viscosity, representing both Newtonian and viscoelastic behaviors. The dispersion curves of attenuation and phase velocity are investigated in function of the above parameters in order to evaluate their sensitivity. The numerical solutions show that the attenuation and phase velocity of surface Love wave are strongly correlated with waveguide thickness and glycerol concentrations. Results also highlighted the substrate thickness effect on the vibration characteristics of the Love wave. Moreover, the Love wave triggers a viscoelastic response in water-glycerol mixtures similar to that of literature. The obtained results are fundamental and can serve as benchmark solution in design of Love wave sensors.

Keywords: Surface Love wave, Viscoelastic fluid, Theoretical approach.

1. Introduction

There is an increasing demand of highly sensitive analytical techniques in the fields of chemistry [1], medical diagnostics [2] and biotechnology [3]. Optical and acoustic waves sensing technologies are currently used [4]. In particular, the Love wave (LW) acoustic sensors have attracted increasing

*Corresponding author

Email address: adil.elbaroudi@ensam.eu (A. El Baroudi)

attention from the scientific community during the last two decades, due to their reported high sensitivity in liquid. Love wave is a transverse surface wave having one component of mechanical displacement, which is parallel to the surface and perpendicular to the direction of wave propagation. The LW sensor is a layered structure formed by a piezoelectric substrate and a guiding layer [5, 6, 7]. In addition, the condition for the existence of Love waves is that the bulk transverse wave velocity in the layer is lower than that in the substrate. The difference between the mechanical properties of the guiding layer and the substrate creates an entrapment of the acoustic energy in the guiding layer keeping the wave energy near the surface [8]. The confinement of the wave in the guiding layer makes Love wave devices very sensitive towards any changes occurring on the sensor surface [9].

The interaction with a viscous fluid was firstly studied in 1992. An exact solution was used to correlate the velocity and attenuation with the viscosity of the fluid [10, 11]. The perturbation theory was also applied to describe the interaction of the acoustic wave with a fluid [12, 13]. This theory gives a comprehensive description regarding the interaction of an acoustic wave in a general layered waveguide structure covered with a thin film which perturbs the mechanical boundary conditions [14]. There are a number of papers concerning the propagation of acoustic surface waves covered with Newtonian liquid [6]. Nevertheless, a detailed exact approach of surface Love wave in a guiding layer covered with a viscoelastic fluid is still lacking.

This article describes a novel approach, efficient, and reliable based on the exact theory, to predict the propagation of Love wave in elastic waveguide loaded by a viscoelastic fluid. The effect of fluid viscoelasticity and confinement on the attenuation and phase velocity of surface Love waves are investigated. The obtained results of various investigations on Love wave propagation in this work can provide interesting information, for example, to design Love wave sensors.

2. Physical model description

To describe the waveguide structure that guides Love waves, we consider a three-layer system consisting of a viscoelastic fluid (index f), an elastic surface layer (index 1) and an elastic solid substrate (index 2), see Fig. 1. The elastic substrate occupies the positive space $y > 0$ and has thickness h. The surface layer rests on top of the substrate and has thickness d. On top of that rests the viscoelastic fluid which occupies the negative half-space $y < 0$.

Note that the Love waves exhibit a multimode character, the fundamental mode plays an important role in many application such as NDT and sensors [11]. Accordingly, in this work, the attention is focused on the properties of the fundamental mode of Love waves. In addition, losses in the waveguide and in the substrate are neglected [6]. Surface waves of the Love type have only one shear horizontal component of vibration. As a result, these waves are insensitive to the loading with liquids of zero or negligible viscosity [15]. Therefore the propagation loss is only due to the fluid viscosity.

From the experimental point of view, phase and amplitude characteristics of Love surface waves can be measured in a closed loop configuration by placing Love wave delay line in a feedback circuit of an electrical oscillator. Another possibility is to use a network analyzer. This apparatus provides phase shift and insertion loss of the Love wave sensor due to the load of the sensor with a measured viscoelastic fluid. The typical frequency range used by Love wave sensors is from 50 MHz to 500 MHz [15].

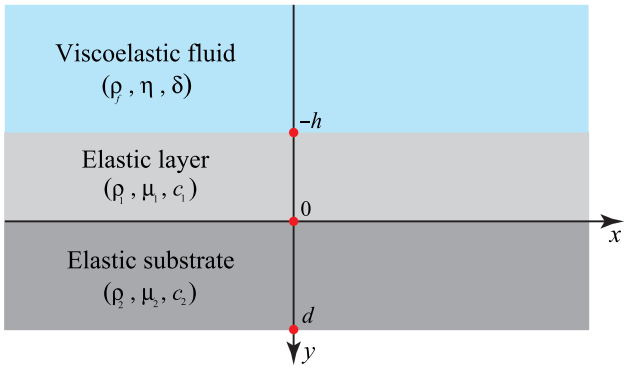

Figure 1: The model geometry. The surface layer (index $i = 1$) and the substrate (index $i = 2$) are elastic solids. ρ_i and μ_i correspond to the density and shear modulus of the elastic mediums. The surface layer is loaded by a viscoelastic fluid. The boundary between the elastic solids is at $y = 0$, with a free surface at $y = d$. The boundary between the surface layer and viscoelastic fluid is at $y = -h$. Love wave propagates in the x-direction and displacement in the z-direction (z is directed out from the paper). For viscoelastic fluid, ρ_f, η and δ are, respectively, density, dynamic viscosity and relaxation time.

2.1. Surface layer and substrate

Continuum mechanics is used to derive a general solution for a Love wave propagating on the surface layer and the elastic substrate. Note that for a waveguide with a typical size of six micrometers the atomic spacing is

sufficiently small that a continuum concept is valid [16]. The displacement field of the Love wave penetrates into the surface layer, requiring a matching of solutions at the boundaries. The Love wave is taken to propagate in the x-direction, with shear displacement in the z-direction (Fig. 1). When we consider a plane harmonic wave in the x-direction ($\exp[j(kx-\omega t)]$), with displacement in z-direction only, $\mathbf{u}_i = (0, 0, w_i)$, and note that, due to symmetry, the displacement should be independent of z, $w_i = w_i(x, y)$. Therefore, the displacement field is governed by the Navier's equation

$$\left(\frac{\partial^2}{\partial x^2} + \frac{\partial^2}{\partial y^2}\right) w_i + \frac{\omega^2}{c_i^2} w_i = 0 \tag{1}$$

where $c_i = \sqrt{\mu_i/\rho_i}$ is the bulk shear wave velocity in the solid media ($i = 1, 2$). Note that time-harmonic dependence $e^{-j\omega t}$ is omitted for simplicity.

2.2. Viscoelastic fluid

In order to describe the viscoelasticity of the fluid medium, the Maxwell model is employed. In a Maxwell fluid, the viscoelastic behavior is modeled as a purely viscous damper and a purely elastic spring connected in series. Since harmonic solutions are sought for the velocity and the shear stress should have the same time dependence, $e^{-j\omega t}$. Thus, the fluid motion is only produced by wave propagation in the surface layer. Furthermore, since only shear deformation arises during transverse waves propagation, we can also ignore the pressure gradient. In addition, the linearized Navier-Stokes equation governs the viscoelastic fluid motion and it can be simplified to the following

$$\nabla \cdot \boldsymbol{\tau} + j\omega\rho_f \mathbf{v} = 0 \tag{2}$$

where $\mathbf{v}$ is the velocity vector, ρ_f is the density and $\boldsymbol{\tau}$ is the shear stress tensor. Therefore, the differential equation for the relation between force and deformation can be written as [17]

$$(1 - j\omega\delta)\,\boldsymbol{\tau} = 2\eta\boldsymbol{\varepsilon}(\mathbf{v}) \tag{3}$$

where δ is the relaxation time, η is the dynamic viscosity and $\boldsymbol{\varepsilon}$ is the strain rate tensor. Applying the divergence operator to both sides of Eq. (3) and taking into account Eq. (2), we get the following viscoelastic fluid equation expressed in terms of the axial component of the velocity field

$$\left(\frac{\partial^2}{\partial x^2} + \frac{\partial^2}{\partial y^2}\right) w_f + \frac{j\omega\rho_f}{\eta}(1 - j\omega\delta)\, w_f = 0 \tag{4}$$

where w_f is the velocity in the z-direction.

2.3. General solution of wave equations

For a plane wave propgation in the x-direction, with displacement in z-direction only, the solution of Eqs. (1) and (4) of the velocity w_f in the viscoelastic fluid and of the displacement w_i in the elastic solids (surface layer and substrate) are sought in the form

$$\left\{ \begin{array}{c} w_f \\ w_i \end{array} \right\}(x,y) = \left\{ \begin{array}{c} W_f(y) \\ W_i(y) \end{array} \right\} e^{jkx} \tag{5}$$

where $k = k_0 + j\alpha$ is the complex wave number. Note that the real part of the wave number k_0 determines the Love wave phase velocity, and the imaginary part α represents the Love wave attenuation. After substitution of Eq. (5) into Eqs. (1) and (4), the y dependence can be expressed as

$$\begin{aligned} W_1(y) &= A_1 \cos(\beta_1 y) + B_1 \sin(\beta_1 y) \\ W_2(y) &= A_2 e^{-\beta_2 y} + B_2 e^{\beta_2 y} \\ W_f(y) &= A_f e^{\beta_f y} \end{aligned}$$

where A_1, B_1, A_2, B_2 and A_f are arbitrary amplitudes and β_1, β_2 and β_f being the vertical wavenumbers

$$\beta_1 = \sqrt{\frac{\omega^2}{c_1^2} - k^2}\ ,\ \beta_2 = \sqrt{k^2 - \frac{\omega^2}{c_2^2}}\ ,\ \beta_f = \sqrt{k^2 - \frac{j\omega\rho_f}{\eta}(1 - j\omega\delta)}$$

Note that when $\omega\delta \ll 1$, the fluid exhibits purely viscous behavior and β_f becomes $\xi = \sqrt{k^2 - j\omega\rho_f/\eta}$.

To assure that the Love wave amplitude in viscoelastic fluid decays to zero with increasing distance from the waveguide surface $y \to -\infty$, $\mathrm{Re}(\beta_f)$ must be greater than zero. In addition, the shear stress components that will be used in boundary and interface conditions are given by

$$\left\{ \begin{array}{c} \sigma_{yz}^{(f)} \\ \sigma_{yz}^{(i)} \end{array} \right\} = \left\{ \begin{array}{c} \dfrac{\eta}{1 - j\omega\delta}\partial_y w_f \\ \mu_i \partial_y w_i \end{array} \right\} = \left\{ \begin{array}{c} \dfrac{\eta}{1 - j\omega\delta}\Sigma_f(y) \\ \mu_i \Sigma_i(y) \end{array} \right\} e^{jkx} \tag{6}$$

where the y dependence is defind as

$$\begin{aligned} \Sigma_1(y) &= \beta_1 \left[B_1 \cos(\beta_1 y) - A_1 \sin(\beta_1 y) \right] \\ \Sigma_2(y) &= \beta_2 \left(B_2 e^{\beta_2 y} - A_2 e^{-\beta_2 y} \right) \\ \Sigma_f(y) &= A_f \beta_f e^{\beta_f y} \end{aligned}$$

2.4. Complex dispersion relation

In this paragraph suitable boundary and interface conditions must now be used to relate solutions in different layers to each other. Accordingly, assuming traction-free outer substrate surface, one can write :

1. At the interface between the viscoelastic fluid and the surface layer ($y = -h$), the velocity and shear stress should be equal

$$\left(w_f - \frac{\partial w_1}{\partial t}\right)_{y=-h} = 0 \tag{7}$$

$$\left[\sigma_{yz}^{(f)} - \sigma_{yz}^{(1)}\right]_{y=-h} = 0 \tag{8}$$

2. At the interface between the surface layer and the substrate ($y = 0$), the displacement and shear stress should be equal

$$\left(w_1 - w_2\right)_{y=0} = 0 \tag{9}$$

$$\left[\sigma_{yz}^{(1)} - \sigma_{yz}^{(2)}\right]_{y=0} = 0 \tag{10}$$

3. These conditions are not sufficient in order to have a fully described system. To complete the boundary conditions, for a substrate, the traction-free outer surface ($y = d$) is assumed

$$\sigma_{yz}^{(2)}\big|_{y=d} = 0 \tag{11}$$

Eqs. (7)-(11) show the boundary and interface conditions between viscoelastic fluid, surface layer and substrate, and Eq. (5) gives the general solutions. Substituting this equation and Eq. (6) into Eqs. (7)-(11) provides five linear and homogeneous equations for the arbitrary constants A_f, A_1, B_1, A_2 and B_2. This system of equations has a nontrivial solution if the determinant of the coefficients equals zero. This leads to the following complex dispersion relation

$$\mu_1\beta_1\left[\frac{j\omega\eta\beta_f}{1-j\omega\delta} - \mu_2\beta_2\tanh\left(\beta_2 d\right)\right] + \left[\mu_1^2\beta_1^2 + \frac{j\omega\eta\beta_f}{1-j\omega\delta}\mu_2\beta_2\tanh\left(\beta_2 d\right)\right]\tan\left(\beta_1 h\right) = 0 \tag{12}$$

Since this relation contains k, ω, as well as all material and geometrical parameters of the viscoelastic fluid, surface layer and substrate, Eq. (12)

represents the implicit complex dispersion relation of Love waves propagating in an elastic surface layer loaded with a viscoelastic fluid. Eq. (12) was solved using Mathematica software. After finding the real part k_0 and the imaginary part α of the wavenumber, the Love wave phase velocity $v = \omega/k_0$ and Love wavelength $\lambda = 2\pi/k_0$ can be calculated. While the root α represents the Love wave attenuation in the direction of propagation.

For a semi-infinite substrate, the complex dispersion relation (12) becomes

$$\mu_1\beta_1\left(\frac{j\omega\eta\beta_f}{1-j\omega\delta}-\mu_2\beta_2\right)+\left(\mu_1^2\beta_1^2+\frac{j\omega\eta\beta_f}{1-j\omega\delta}\mu_2\beta_2\right)\tan\left(\beta_1 h\right)=0 \qquad (13)$$

For a viscous Newtonian fluid, the complex dispersion relation (13) becomes

$$\mu_1\beta_1\left(j\omega\eta\xi-\mu_2\beta_2\right)+\left(\mu_1^2\beta_1^2+j\omega\eta\xi\mu_2\beta_2\right)\tan\left(\beta_1 h\right)=0 \qquad (14)$$

which was previously obtained by [6, 18].

3. Results and discussion

The material properties given in Table 1 for viscoelastic fluid and which are used by Mitsakakis *et al.* [5] were taken to construct this numerical example. The material properties were derived from [4] for the waveguide and substrate are given in Table 2. In this work, numerical calculation is performed in the glycerol concentrations range from 15.4% to 88.0% and for three values of frequency 50, 100 and 150 MHz.

Table 3 shows the variations of phase velocity and attenuation at lower glycerol concentration (15.4%) in both Newtonian and Viscoelastic fluid media. This mixture is characterized by a relaxation time of 28 ps (Table 1). Table 3 also shows that the modification of the phase velocity and attenuation by elastic effects is relatively minor in this case, a more significant effect can occur when the glycerol concentration becomes more important. This is due to the low value of the time constant 28 ps and by the resulting values of $\omega\delta$: $8.8\cdot10^{-3}$ (50 MHz), $1.7\cdot10^{-2}$ (100 MHz) and $2.6\cdot10^{-2}$ (150 MHz). These values lead to neglect the term $\omega\delta$ in equation (2) to find the linearized Navier-Stokes equation for a purely Newtonian fluid.

Table 4 shows the variations of phase velocity and attenuation at higher glycerol concentration (88.0%) in both Newtonian and Viscoelastic fluid media. This mixture is characterized by a high relaxation time 2562 ps. From

Table 1: Material parameters used for water-glycerol mixtures. χ is the concentration of glycerol in water.

χ (%)	η (cPa $\cdot$ s)	ρ_f (kg/m^3)	δ (ps)
15.4	1.4	1017	28
25.6	1.7	1029	38
32.9	2.7	1038	54
37.3	3.1	1044	62
42.3	3.8	1050	76
46.7	4.6	1055	92
52.2	5.9	1062	118
62.1	10.2	1075	204
72.0	21.9	1087	438
75.9	33.2	1093	664
80.0	49.5	1098	990
84.0	81.8	1104	1636
88.0	128.1	1109	2562

this table, we can see that the elastic effects become significant on the obtained results. This is due to the high value of the time constant 2562 ps and by the resulting values of $\omega\delta$: 0.8 (50 MHz), 1.6 (100 MHz) and 2.4 (150 MHz). Contrary to what has been envisaged for a low Glycerol concentration, these values do not make it possible to neglect the term $\omega\delta$ in equation (2).

3.1. Substrate thickness effect

We first examine the relative importance of the substrate thickness effect on the phase velocity and attenuation. The relative importance is characterized by comparing the phase velocity and attenuation when finite substrate is considered ($_{\mathrm{f}}$) to the phase velocity and attenuation when the substrate is assumed to be semi-infinite ($_{\mathrm{sf}}$). The normalized phase velocity ($v_{\mathrm{f}}/v_{\mathrm{sf}}$) and attenuation ($\alpha_{\mathrm{f}}/\alpha_{\mathrm{sf}}$) should approach unity when the substrate thickness effect is negligible and decrease as the substrate thickness effect becomes significant. Figures 2 and 3 illustrate the substrate thickness effect on the phase velocity and attenuation for two water-glycerol mixtures and two values of

Table 2: Material parameters used for surface layer and substrate.

	ρ_i (kg/m^3)	μ_i (Pa)	c_i (m/s)
Surface layer ($i = 1$)	8900	3.91×10^{10}	2096
Substrate ($i = 2$)	2600	5.80×10^{10}	4723

Table 3: Phase velocity v and attenuation α with $h = 1$ (μm) in the case of viscous and viscoelastic water-glycerol mixture media (15.4 %).

	Viscous		Viscoelastic	
Frequency	v	α	v	α
(MHz)	(m/s)	(Np/m)	(m/s)	(Np/m)
50	4645.40	14.65	4645.40	14.72
100	4438.05	78.79	4438.07	79.47
150	4157.36	201.08	4157.41	203.67

frequencies. The normalized phase velocity and attenuation rapidly increase for the low values of substrate thickness and then reach a plateau region. The thickness values allowing access to the plateau region are equal to 0.06 mm (50 MHz) and 0.021 mm (100 MHz). These values are much lower than the typical thickness (0.5 mm) of Quartz substrates used in design of Love wave sensors [5]. The substrate of these sensors can thus be considered to be a semi-infinite medium and the complex dispersion equation (11) can be used. These results can be interpreted as follows : when the substrate thickness is greater than the penetration depth of the Love wave, the substrate can be considered as infinite medium. Otherwise, if the thickness of this substrate is lower than the penetration depth of the Love wave, loss of energy occurs. Therefore, the phase velocity and attenuation decrease. This phenomenon is linked to the the frequency because the depth penetration decreases with increasing frequency.

Table 4: Phase velocity v and attenuation α with $h = 1$ (μm) in the case of viscous and viscoelastic water-glycerol mixture media (88.0 %).

	Viscous		Viscoelastic	
Frequency	v	α	v	α
(MHz)	(m/s)	(Np/m)	(m/s)	(Np/m)
50	4636.44	155.15	4641.35	169.53
100	4416.11	820.56	4434.11	783.36
150	4124.72	2080.38	4155.27	1725.95

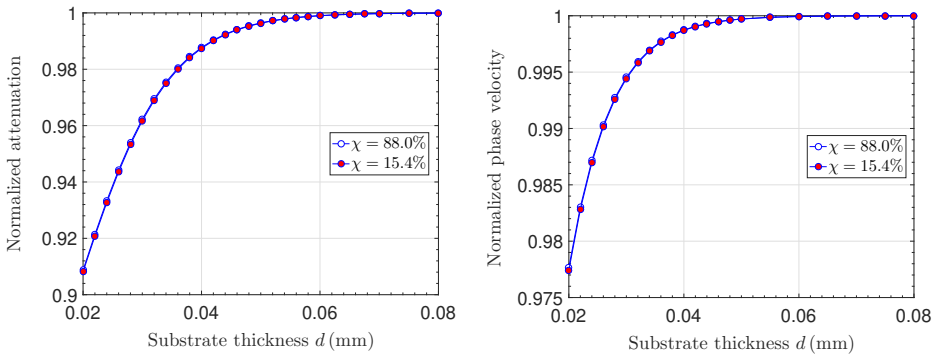

Figure 2: Normalized attenuation and phase velocity versus substrate thickness for $f = 50$ (MHz).

3.2. Penetration depth effect

The estimation of the penetration depth of wave in fluid is fundamental when the Love wave sensor is intended to characterize viscoelastic fluids. In this article, we define the penetration depth as $\sqrt{2\eta/(\rho_f\omega)}$, which is the same as the definition adopted by Martin *et al.* [19]. Figure 4 shows the evolution of the penetration depth as a function of glycerol concentration for three frequencies $50, 100$ and 150 MHz. Figure 4 also shows that the penetration depth remains lower than 0.9 μm. This value is much lower than the typical height of a microfluidic channel 100 μm (see Raimbault *et al.* [20]). The liquid layer can therefore be assimilated to a semi-infinite medium.

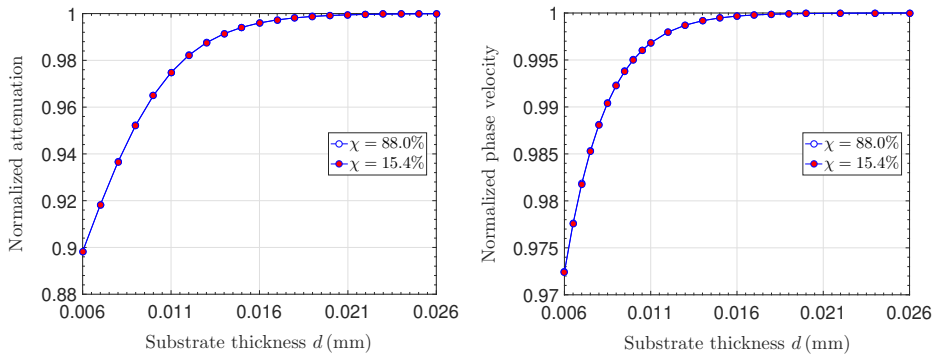

Figure 3: Normalized attenuation and phase velocity versus substrate thickness for $f = 150$ (MHz).

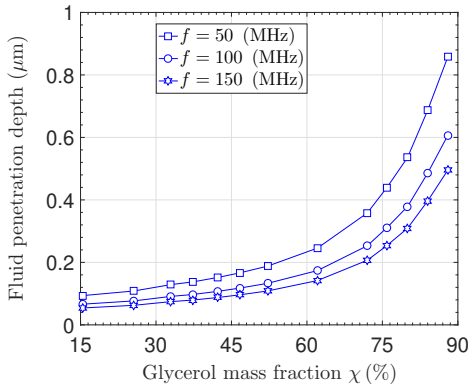

Figure 4: Fluid penetration depth versus glycerol mass fraction.

3.3. Waveguide thickness effect

Figure 5(a) illustrates the influence of the waveguide (surface layer) thickness on the Love wave attenuation for four water-glycerol mixtures at frequency 50 MHz. The Love wave attenuation first increases with the waveguide thickness to reach a maximum value of 7 μm ($h/\lambda = 0.11$) and then starts decreasing. The obtained curves are similar to those of sensitivity to the mass effect obtained for a Love wave sensor [11, 21]. This behavior is more significant when the Glycerol concentration increases. To interpret these results, the energy confinement in the waveguide has to be taken into account. Thus, when the waveguide thickness increases, the energy of the Love wave

increases while the energy present in the substrate decreases [8, 11]. This has the effect of increasing wave amplitude at the interface with the liquid. The attenuation due to the viscoelastic properties of the liquid thus becomes stronger.

The influence of the waveguide thickness on the phase velocity is shown in figure 5(b) for two water-glycerol mixtures at a frequency of 50 MHz. The phase velocity decreases as the thickness increases from 0 to 10 μm. When the thickness tends to 0 the phase velocity tends toward the wave velocity in the substrate. As the thickness increases, the phase velocity tends asymptotically toward the wave velocity in the waveguide. This is in agreement with previously published experimental results [9]. The confinement concept can justify this behavior. When the thickness of the waveguide tends to 0, the elastic energy is localized in the substrate, it is therefore natural that the phase velocity be equal to the substrate characteristic velocity. When the thickness increases, the confinement of the wave in the guide becomes more important, the phase velocity decreases and tends asymptotically towards the phase velocity in the surface layer. In addition, the influence of the frequency on the decay of the phase velocity can be explained as follows: when the frequency increases the confinement is greater for a given thickness of the guide and the phase velocity is lower.

The effect of the waveguide thickness on the attenuation and phase velocity at frequency 100 MHz is depicted in Figure 6. The comparison of graphs 6 and 5 shows that the frequency increase causes much greater attenuation and phase velocity variations as the thickness of the waveguide increases. This can be physically justified as follows: when the frequency increases, the wave attenuation in substrate is stronger and the confinement becomes more important. Therefore, for a well-defined waveguide thickness the attenuation is higher and the phase velocity is lower. Thus, the figure 7 is obtained choosing a frequency equal to 150 MHz. The observed behaviors are identical to those deduced from the previous figures but more significantly.

3.4. Glycerol concentration effect

In this paragraph, we investigate how the phase velocity and attenuation vary with the glycerol mass fraction in both Newtonian and viscoelastic fluid media. In Fig. 8-10, we study how the vibrations characteristics responses varies with the glycerol mass fraction (i.e., shear viscosity) in both Newtonian and viscoelastic behaviors. By considering a viscous incompressible flow and increasing the glycerol mass fraction, a Newtonian fluid model predicted a

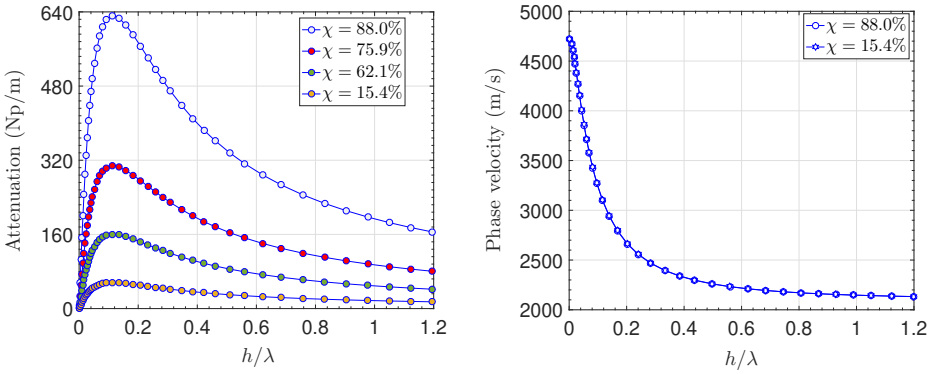

(a) (b)

Figure 5: Attenuation and phase velocity versus normalized surface layer thickness for $f = 50$ (MHz).

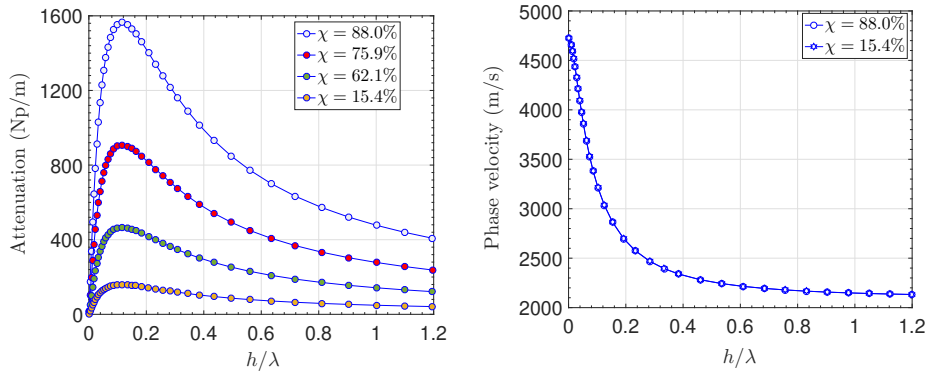

(a) (b)

Figure 6: Attenuation and phase velocity versus normalized surface layer thickness for $f = 100$ (MHz).

monotonically decreasing relationship between the vibrations characteristics responses and the glycerol mass fraction [16]. Fig. 8-10 are in good agreement with this Newtonian behavior. However, a Maxwell model highlighted a non-monotonically decreasing correlation between the phase velocity and glycerol mass fraction: the phase velocity first decreased as the glycerol mass fraction increased, reaching a minimum before increasing again. Therefore we can conclude that the non-monotonic behavior manifested the intrinsic viscoelastic properties of fluid [22, 23].

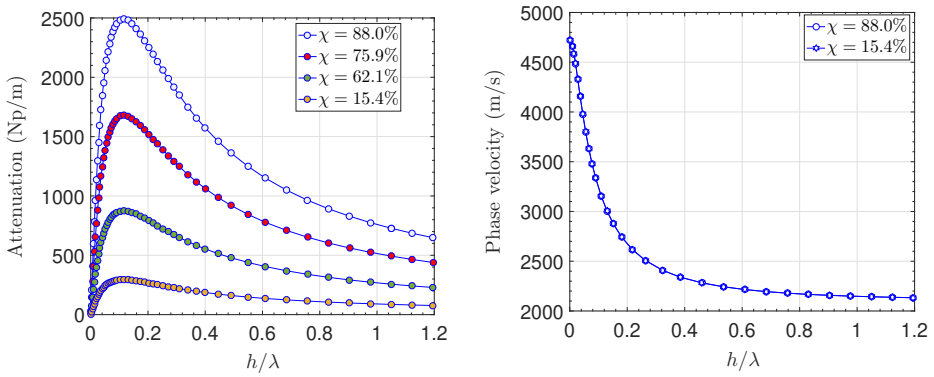

(a) (b)

Figure 7: Attenuation and phase velocity versus normalized surface layer thickness for $f = 150$ (MHz).

Figure 8 shows the variation of phase velocity and attenuation for a frequency equal to 50 MHz and for a waveguide thickness of 7 μm. Note that this thickness value corresponds to a maximum attenuation at the considered frequency (see Fig. 5(a)). The elastic effects are significant for a glycerol concentration greater than 62.1%. For glycerol concentration values less than the critical value (62.1%), the elasticity can be neglected and the behavior is Newtonian [6]. This is due to the time constant value less than 204 ps corresponding to $\omega\delta$ less than 0.064. The term $\omega\delta$ is then negligible compared to 1 and equation 2 can be assimilated to the linearized Navier-Stokes equation characterizing a Newtonian behavior. These observations are in good adequacy with the theoretical and experimental results obtained by an approximate approach based on the perturbation theory [5, 14, 24].

In Figure 9 the phase velocity and attenuation are plotted against glycerol mass fraction for a frequency equal to 100 MHz and for a waveguide thickness of 3.5 μm ($h/\lambda = 0.11$). Note that this thickness value corresponds to a maximum attenuation at the considered frequency (see Fig. 6(a)). The behavior is Newtonian for a concentration lower than 52.2%. This concentration value is associated with a time constant equal to 118 ps and $\omega\delta = 0.074$, which is negligible compared to 1 justifies a Newtonian behavior [5, 24].

Figure 10 illustrates the variation of phase velocity and attenuation for a frequency equal to 150 MHz and for a waveguide thickness of 2.4 μm ($h/\lambda = 0.11$). Note that this thickness value corresponds to a maximum

attenuation at the considered frequency (see Fig. 7(a)). The behavior is Newtonian for a concentration lower than 46.7%. This concentration value is associated with a time constant equal to 92 ps and $\omega\delta = 0.086$. For this last value, the behavior is Newtonian.

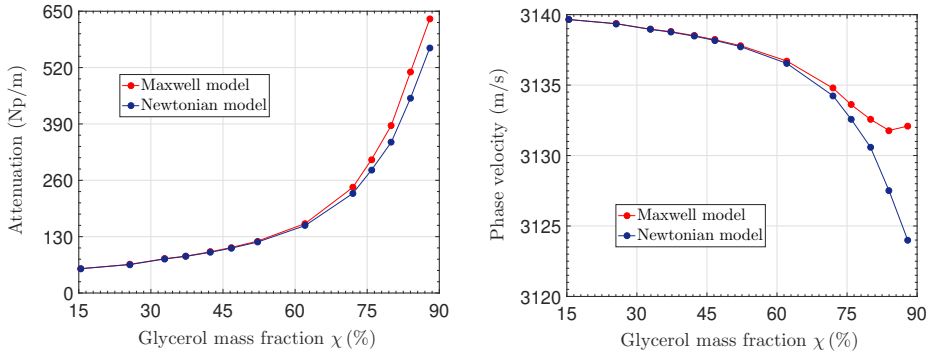

(a) (b)

Figure 8: Attenuation and phase velocity versus glycerol mass fraction with $h = 7$ (μm) and $f = 50$ (MHz).

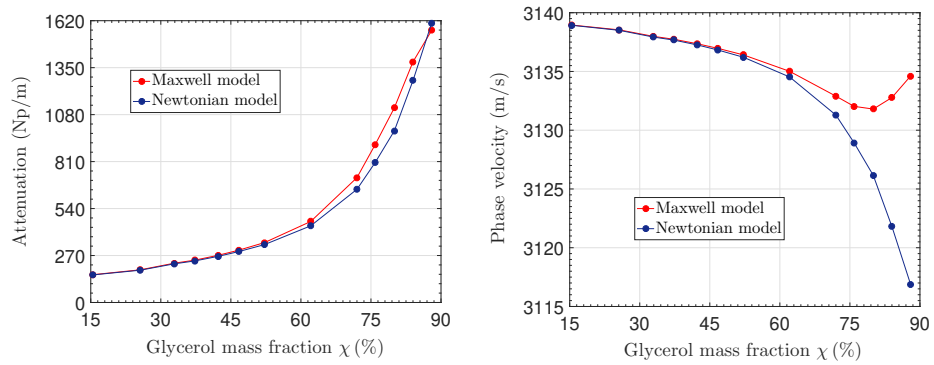

(a) (b)

Figure 9: Attenuation and phase velocity versus glycerol mass fraction with $h = 3.5$ (μm) and $f = 100$ (MHz).

4. Conclusions

Propagation of surface Love wave in elastic waveguide loaded on its surface with a viscoelastic fluid is investigated using a new original approach

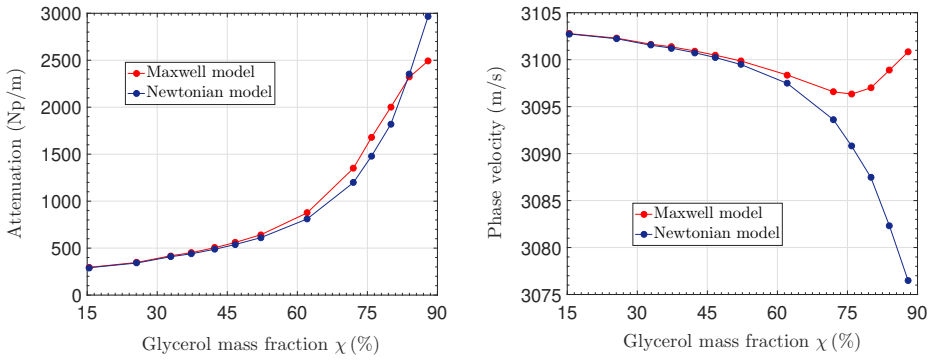

(a) (b)

Figure 10: Attenuation and phase velocity versus glycerol mass fraction with $h = 2.4$ (μm) and $f = 150$ (MHz).

based on the exact theory in this paper. A new theoretical form of the complex dispersion relation was developed. Therefore, the graphs highlighting the behavior of attenuation and phase velocity of Love waves versus waveguide thickness and glycerol concentrations were obtained. Three detailed dispersion relations were established, (i) viscoelastic fluid with finite substrate, (ii) viscoelastic fluid with semi-infinite substrate, and (iii) Newtonian fluid with semi-infinite substrate. The last dispersion relation was previously obtained by [6, 18]. Finally, the new original theoretical resolution proposed in this work can be used to develop and design the Love wave sensors.

[1] F. Josse, F. Bender and R. W. Cernose. Guided shear horizontal surface acoustic wave sensors for chemical and biochemical detection in liquids, Anal. Chem. **73**(24), 5937–5944 (2001).

[2] F. Zhang, S. Li, K. Cao, P. Wang, Y. Su, X. Zhu and Y. Wan. A Microfluidic Love-Wave Biosensing Device for PSA Detection Based on an Aptamer Beacon Probe, Sensors **15**(6), 13839–13850 (2015).

[3] D. Matatagui, J. L. Fontecha, M. J. Fernandez, I. Gracia, C. Cane, J. P. Santos and M. C. Horrillo. Love-Wave sensors combined with Microfluidics for fast detection of biological Warfare agents, Sensors **14**(7), 12658–69 (2014).

[4] M. I. G. Rocha, Y. Jimenez, F. A. Laurent and A. Arnau. Love Wave Biosensors: A Review, IntechOpen 277–310 (2013).

[5] K. Mitsakakis, A. Tsortos, J. Kondoh and E. Gizeli. Parametric study of SH-SAW device response to various types of surface perturbations, Sensors and Actuators B: Chemical **138**, 408–416 (2009).

[6] P. Kielczynski, M. Szalewski, A. Balcerzak. Effect of a viscous liquid loading on Love wave propagation, International Journal of Solids and Structures **49**(17), 2314–2319 (2012).

[7] A. El Baroudi. Influence of Poroelasticity of the Surface Layer on the Surface Love Wave Propagation, Journal of Applied Mechanics **85**, 051002-1–7 (2018).

[8] G. Kovacs and A. Venema. Theoretical comparison of sensitivities of acoustic shear wave modes for (bio) chemical sensing in liquids, Applied Physics Letters **61**(6) (1992).

[9] J. Du, G. L. Harding, J. A. Ogilvy, P. R. Dencher and M. Lake. A study of Love-wave acoustic sensors, Sensors and Actuators A: Physical **56** (3), 211–219 (1996).

[10] J. O. Kim. The effect of a viscous fluid on Love waves in a layered medium, The Journal of the Acoustical Society of America **91**(6), 3099–3103 (2014).

[11] S. Li, Y. Wan, C. Fan and Y. Su. Theoretical Study of Monolayer and Double-Layer Waveguide Love Wave Sensors for Achieving High Sensitivity, Sensors **17**(3) (2017).

[12] G. Kovacs, M. J. Vellekoop, R. Haueis, G. W. Lubking and A. Venema. A love wave sensor for (bio)chemical sensing in liquids, Sensors and Actuators A: Physical **43**, 38-43 (1994).

[13] A. Vikstrom and M. V. Voinova. Soft-film dynamics of SH-SAW sensors in viscous and viscoelastic fluids, Sensing and Bio-Sensing Research **11**(2), 78–85 (2016).

[14] B. A. Auld. Acoustic fields and waves in solids, A Wiley-Interscience publication (1973).

[15] P. Kielczynski. Surface Waves - New Trends and Developments, Properties and Applications of Love Surface Waves in Seismology and Biosensors, IntechOpen 17–31 (2018).

[16] D. Chakraborty, E. V. Leeuwen, M. Pelton and J. E. Sader. Vibration of nanoparticles in viscous fluids, J. Phys. Chem. C **117**(16), 8536–8544 (2013).

[17] D. D. Joseph. Fluid Dynamics of viscoelastic liquids, Springer (1990).

[18] C. Caliendo, S. Sait and F. Boubenider. Love-Mode MEMS Devices for Sensing Applications in Liquids, Micromachines **7**(1) (2016).

[19] S. J. Martin, A. J. Ricco, T. M. Niemczyk and G. C. Frye. Characterization of SH acoustic plate mode liquid sensors, Sensors and Actuators **20**(3), 253–268 (1989).

[20] V. Raimbault, D. Rebière, C. Dejous, M. Guirardel and V. Conedera. Acoustic Love wave platform with PDMS microfluidic chip, Sensors and Actuators A: Physical **142**(1), 160–165 (2008).

[21] C. McMullan, H. Mehta, E. Gizeli, H. Mehta and C. R. Lowe. Modelling of the mass sensitivity of the Love wave device in the presence of a viscous liquid, Journal of Physics D: Applied Physics **33**(23), 3053–3059 (2000).

[22] M. Pelton, D. Chakraborty, E. Malachosky, P. Guyot-Sionnest and J. E. Sader. Viscoelastic Flows in Simple Liquids Generated by Vibrating Nanostructures, Phys. Rev. Lett. **111**, 244502 (2013).

[23] V. Galstyan, O. S. Pak and H. A. Stone. A note on the breathing mode of an elastic sphere in Newtonian and complex fluids, Phys. Fluids **27**, 032001 (2015).

[24] B. Jakoby and M. J. Vellekoop. Viscosity sensing using a Love-wave device, Sensors and Actuators A: Physical **68**, 275–281 (1998).